

# **Diffuse, Monoenergetic, and Broadband (wave) Aurora: Relative Precipitating Energy Flux**

P. T. Newell, T. Sotirelis, and S. Wing  
The Johns Hopkins University  
Applied Physics Laboratory  
Laurel, Maryland, 20723

# Types of Auroral Precipitation

## **Discrete** (*electron acceleration*)

--Monoenergetic: Most of the energy flux is in one or two DMSP channels.

Source: quasi-static electric fields

--Broadband: Electron acceleration over three or more DMSP channels.

Source: Dispersive Alfvén waves (DAWs).

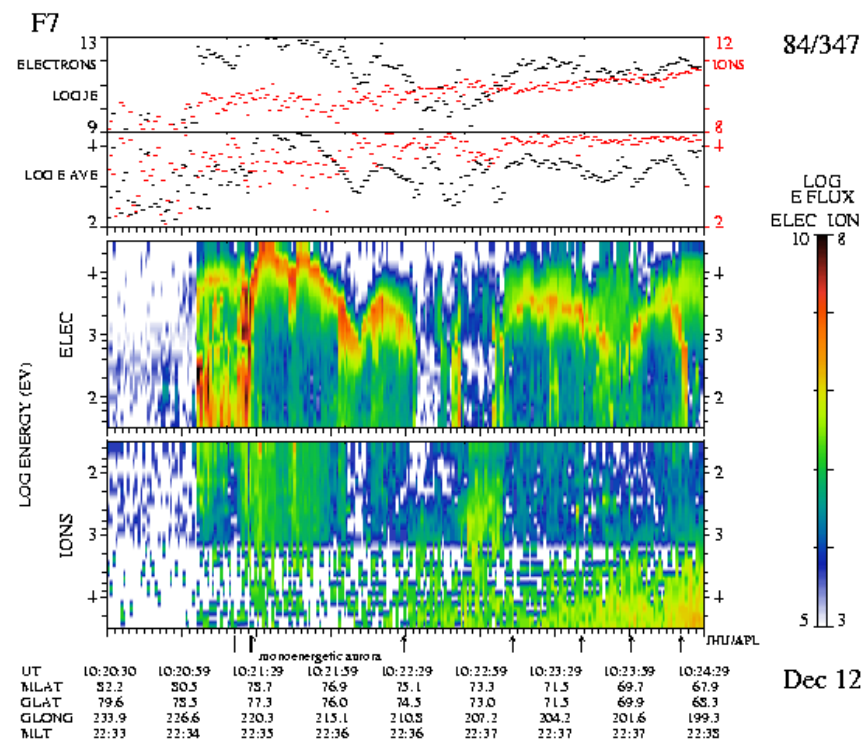
## **Diffuse** (*unaccelerated*)

--Electron

--Ion

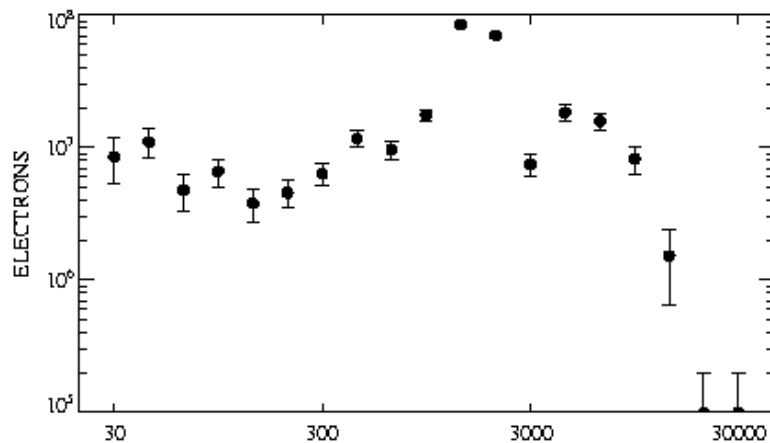
Most of the energy flux is e-, because the light e- mass (and thus high  $v$ ) outweighs the higher ion energy density

# Example Of Monoenergetic Aurora

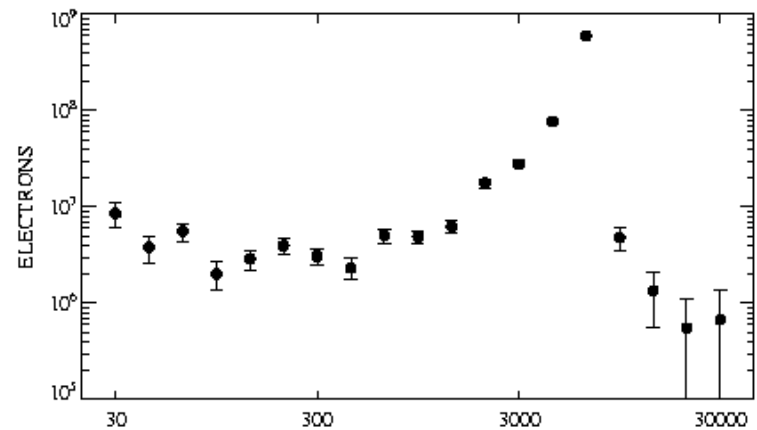


# Examples of Monoenergetic Peaks

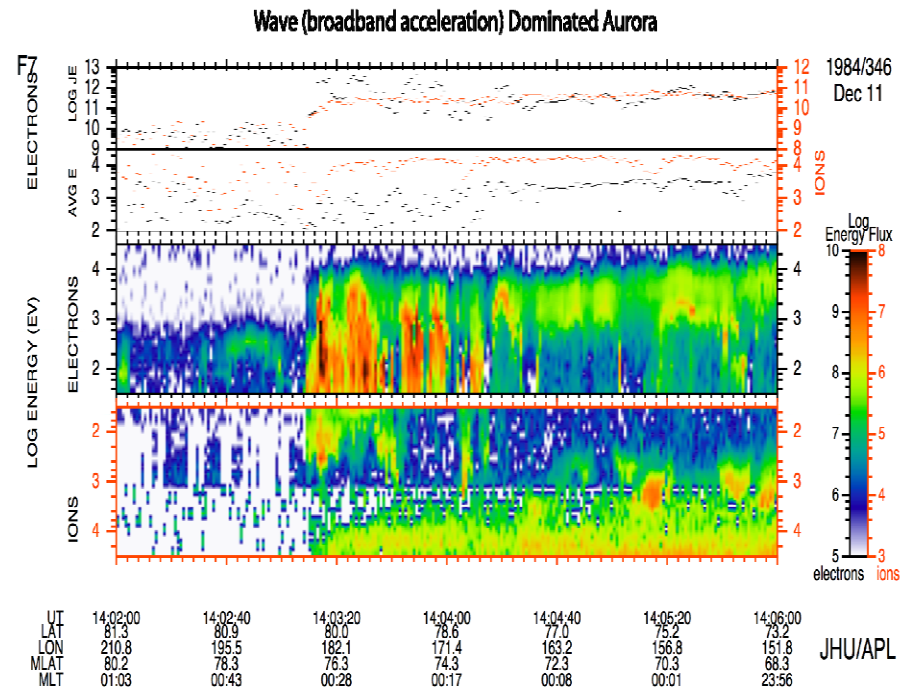
DMSP F13 1996/166 02:07:44



DMSP F12 1996/169 01:31:24

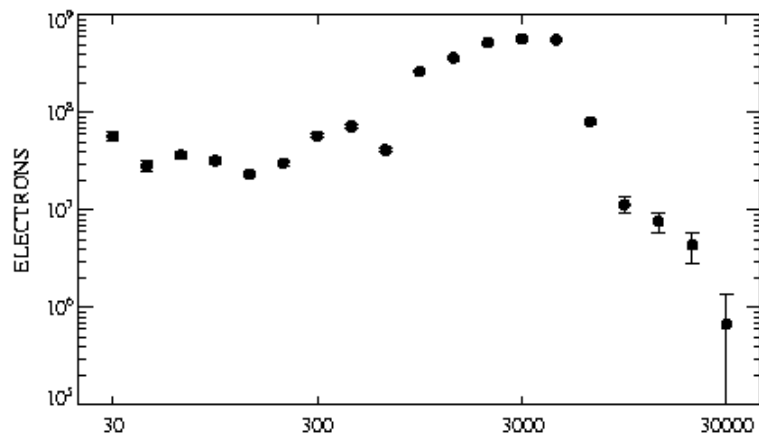


# Example of Broadband Dominated Aurora



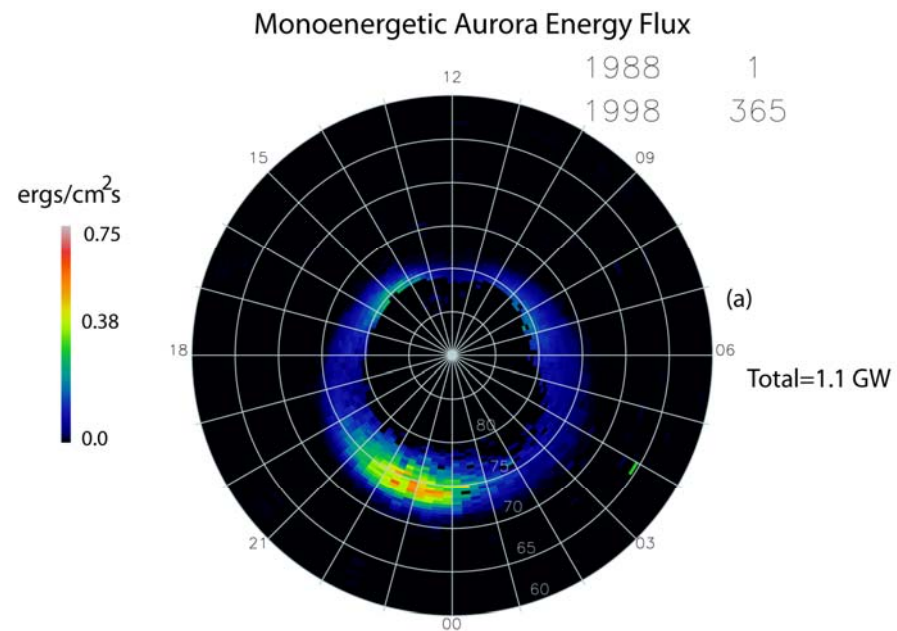
# Broadband Electron Acceleration

DMSP F12 1996/170 23:24:54

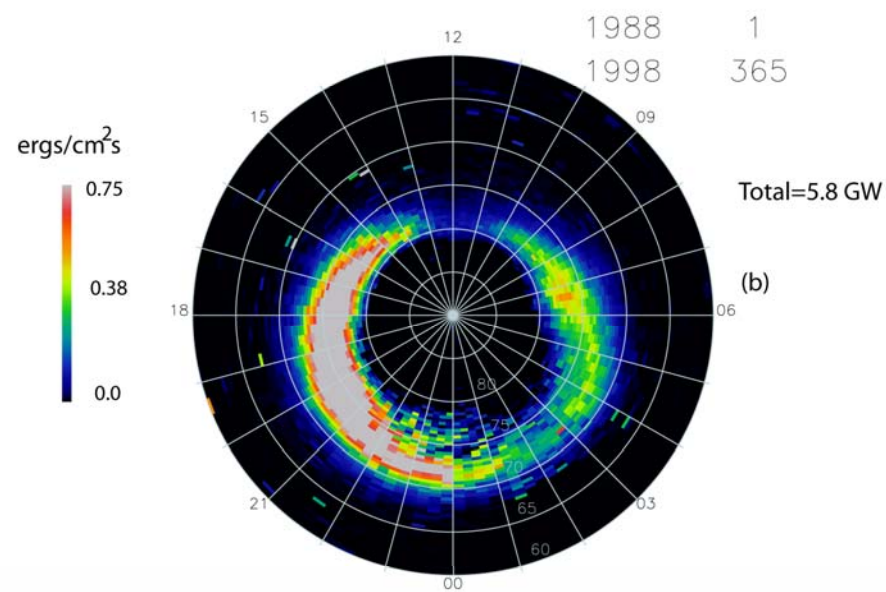


# Criteria for Sorting Auroral Types

- *Accelerated* (or “discrete”) if 1 or more channel has  $dj_E/dE > 10^8 \text{ eV/cm}^2 \text{ s str eV}$  (necessary but not sufficient condition)
- *Monoenergetic* (quasi-static electric fields) if only 1 or 2 channels dominate (factor of 5 > other channels)
- *Broadband* (“wave”) if 3 or more channels are  $> 2 \times 10^8 \text{ eV/cm}^2 \text{ s str eV}$



Low Solar Wind  
Driving



High Solar Wind  
Driving

9632 Satellite-days

Figure 3. Monoenergetic hemispheric energy flux for conditions of (a) low and (b) high solar wind driving.

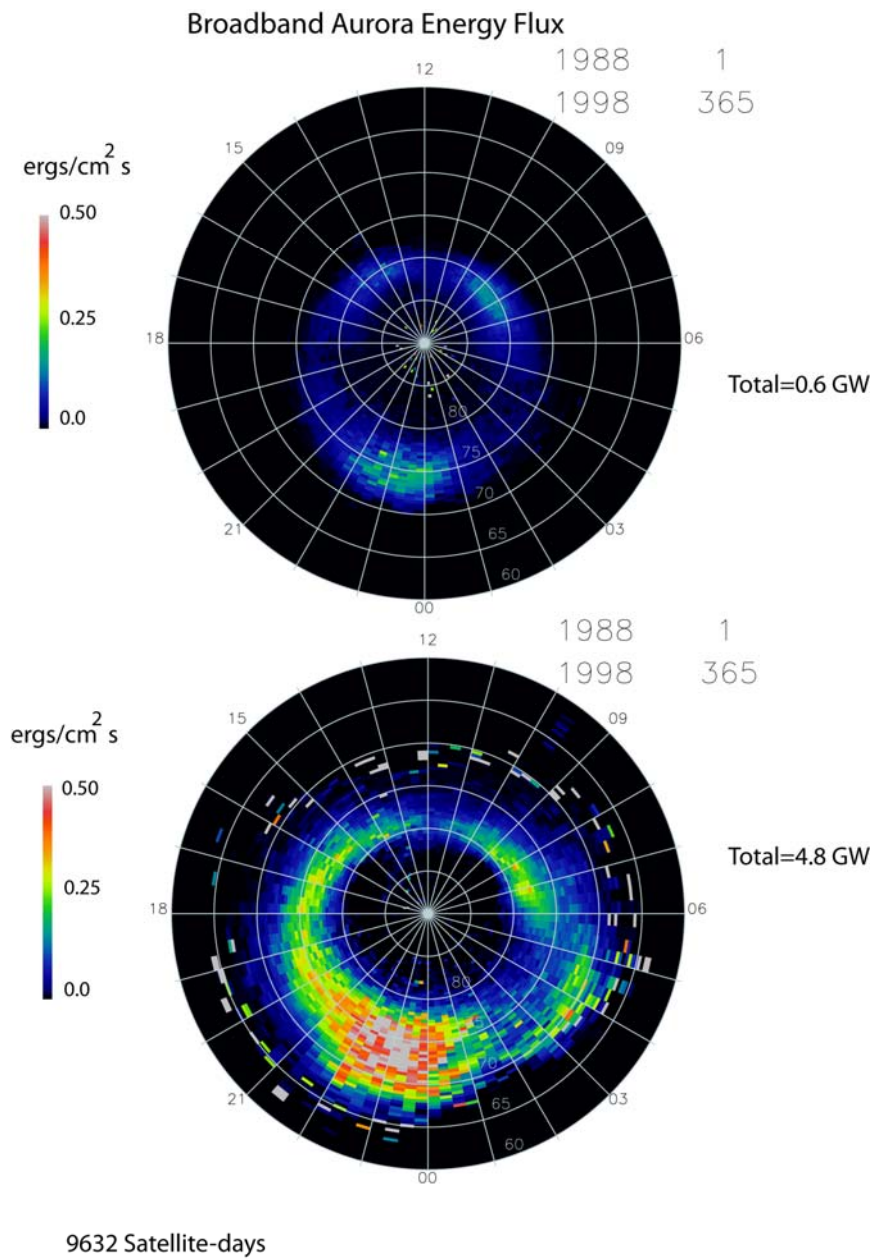


Figure 4. Broadband acceleration hemispheric energy flux for (a) low and (b) high solar wind driving.

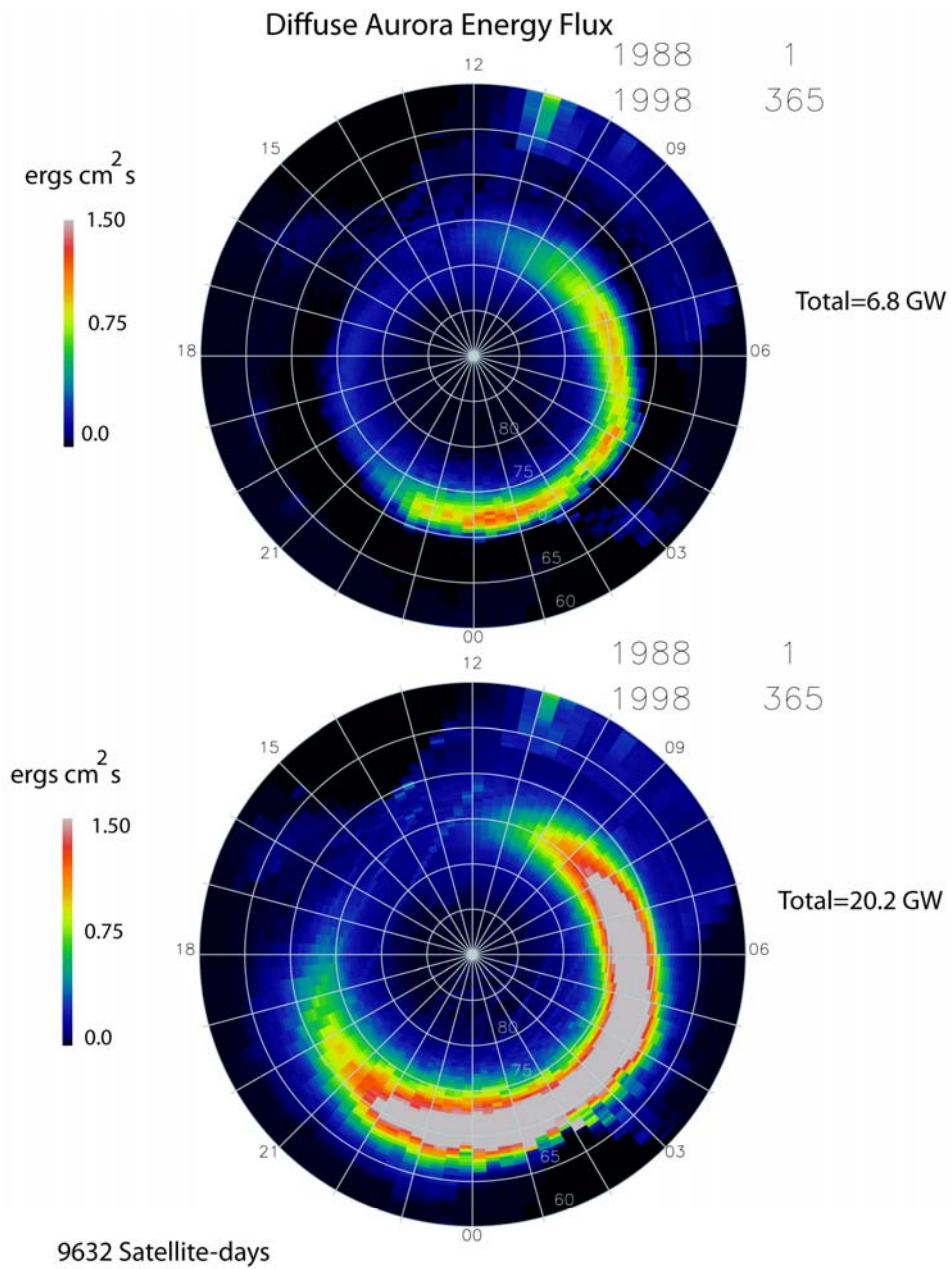


Figure 5. Diffuse electron aurora hemispheric energy flux for (a) low and (b) high solar wind driving.

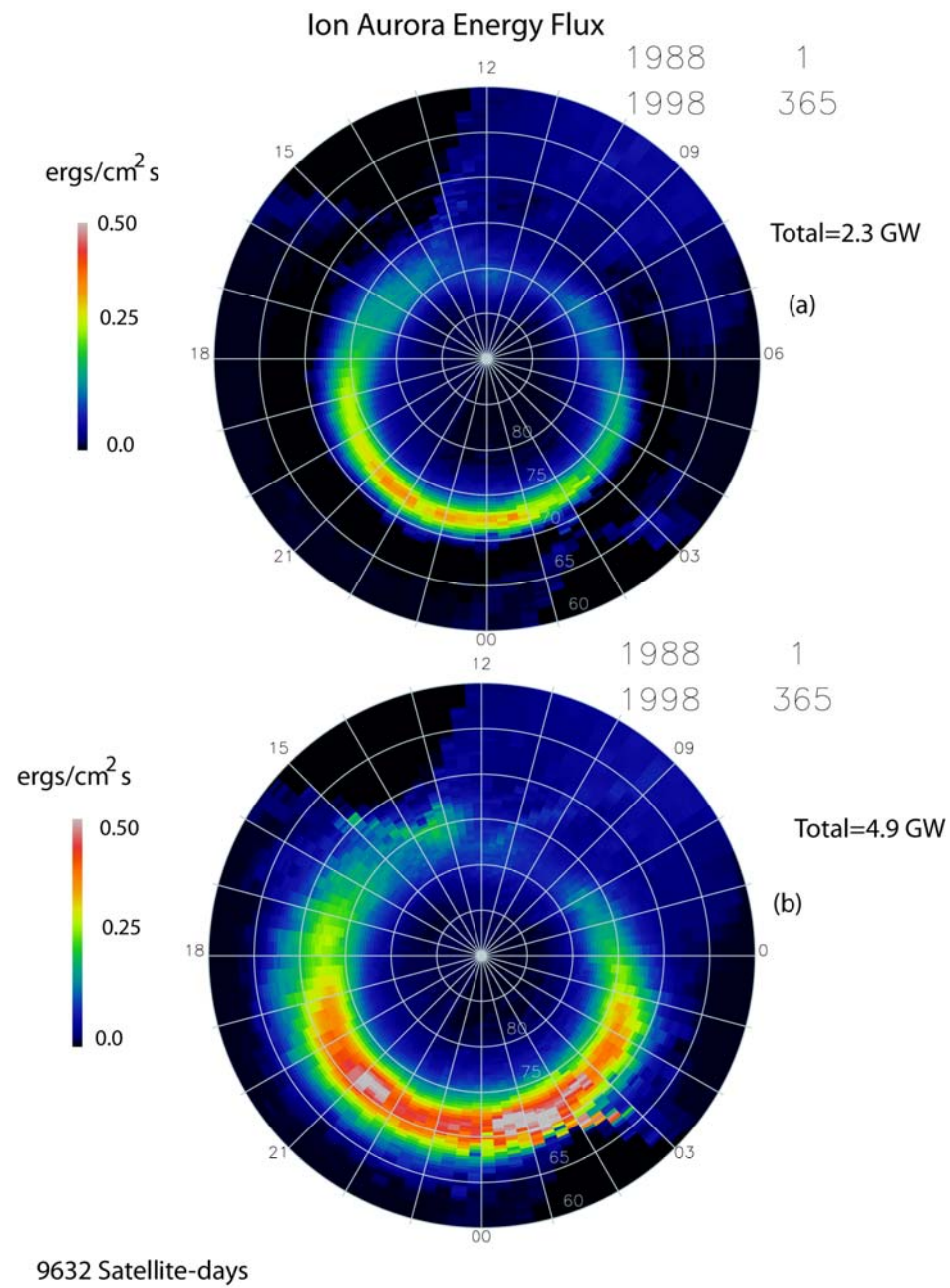


Figure 6. Ion aurora hemispheric energy flux for (a) low and (b) high solar wind driving.

# Parameterization

- Functional fit versus solar wind (rather than bins)
- Each type of aurora fitted separately
- Each MLT/MLAT bin fitted separately
- Solar wind driving based on

$$d\Phi_{\text{MP}}/dt = v^{4/3} B_T^{2/3} \sin^{8/3}(\theta c/2)$$

“Low” (or quiet) here is  $0.25 \langle d\Phi_{\text{MP}}/dt \rangle$

“High” (or active) here is  $1.5 \langle d\Phi_{\text{MP}}/dt \rangle$

## Model Construction

4 auroral types x 96 MLT bins x 120 MLAT bins = 46,080 regression eqns

$$\text{Auroral power}(\text{mlat\_bin}, \text{mlt\_bin}, \text{aurora\_type}) = a + b * d\Phi_{\text{MP}}/dt$$

The same is done for number flux (46,080 more regressions)

The probability of observing each type of electron aurora is also fit with a similar regression equation.

Ion aurora is all lumped together, so there is no probability fit

Finally energy flux (or number flux) is the product of the probability of observing an aurora times the power (or number flux) when present. This can be evaluated for any solar wind history (the IMF for the last 3 hours is input)

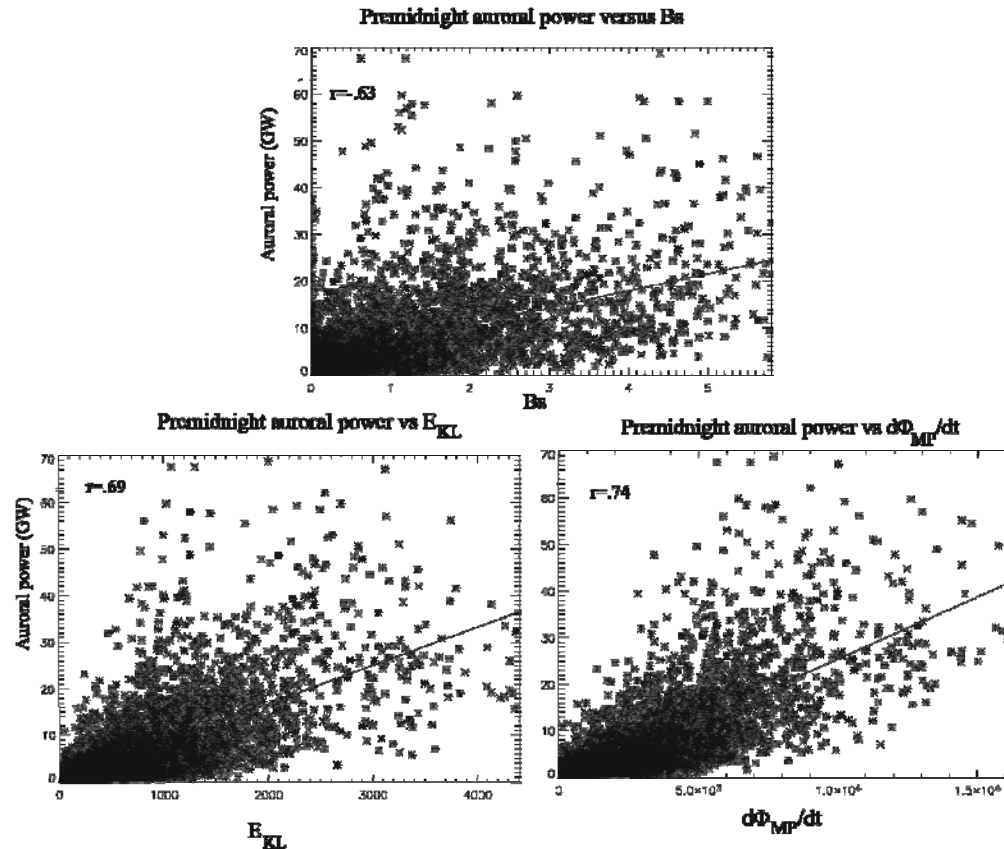


Figure 1. The ability to predict auroral power from solar wind conditions varies greatly according to the coupling function used.  $Bz$  (top) accounts for only 40% of the variance, while the best function, bottom left, accounts for 55%.

Global Auroral Power (from Polar UVI images)  
Can Be Predicted Better Using  $d\Phi_{MP}/dt$

# Relative Contributions to Hemispheric Precipitating Energy Flux

Aurora Type	Hemispheric Power: Quiet (Gigawatts)	Hemispheric Power: Active (Gigawatts)	Hemispheric Power: All Conditions Gigawatts
Diffuse (e-)	6.8 (63%)	20.2 (57%)	12.6 (61%)
Diffuse (ion)	2.3 (21%)	4.9 (14%)	3.4 (16%)
Monoenergetic	1.1 (10%)	5.8 (15%)	3.3 (16%)
Broadband	0.6 (6%)	4.8 (13%)	1.5 (6%)

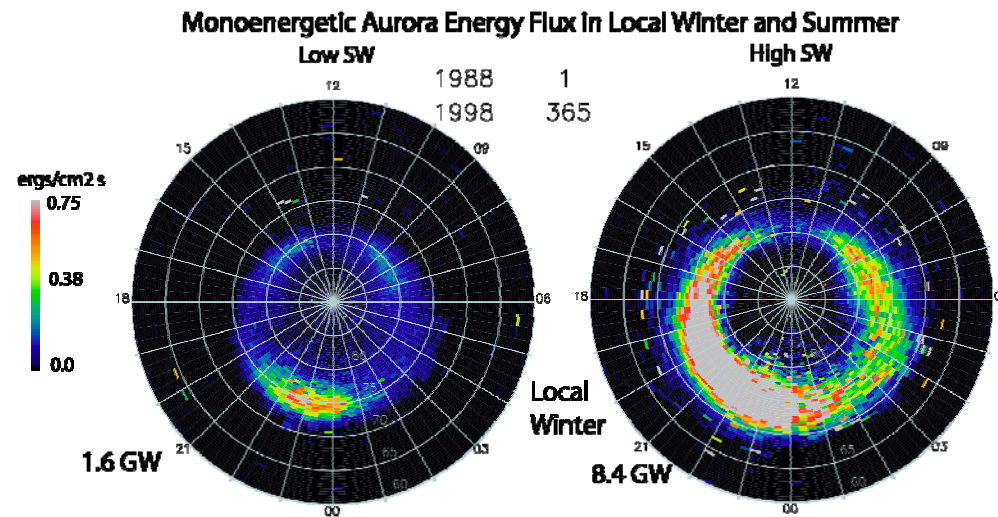
# Number Flux: Relative Contributions

Aurora Type	Low SW Driving	High SW Driving	All Conditions
Diffuse (e-)	$3.2 \times 10^{25}$ (60%)	$5.2 \times 10^{25}$ (48%)	$4.1 \times 10^{25}$ (55%)
Diffuse (ion)	$2.4 \times 10^{24}$ (5%)	$4.1 \times 10^{24}$ (4%)	$3.1 \times 10^{24}$ (4%)
Monoenergetic	$1.1 \times 10^{25}$ (21%)	$2.3 \times 10^{25}$ (21%)	$1.6 \times 10^{25}$ (21%)
Broadband	$7.6 \times 10^{24}$ (14%)	$3.1 \times 10^{25}$ (28%)	$1.5 \times 10^{25}$ (20%)

# Caveats

- Energy flux assumes isotropy within the loss cone – excellent assumption for diffuse aurora, not always true for monoenergetic aurora
- Diffuse aurora extrapolated (from measured 30 keV to 50 keV), assuming Maxwellian. This underestimates ion energy flux.

Winter



Summer

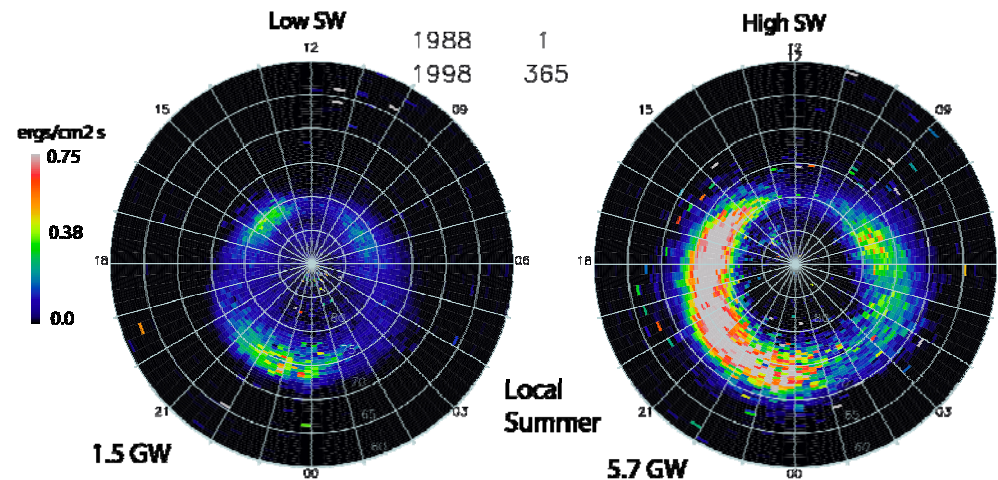


Figure 3. Monoenergetic aurora energy flux for local winter (top two panels) and summer (bottom two). Low solar wind driving is on the left, high driving on the right.

## Why a New Generation Precipitation Model?

- Each of the four types of aurora have different solar wind driving (or substorm cycle or Kp) dependence
- Monoenergetic aurora has a strong seasonal dependence (winter/summer = 1.70), diffuse, wave moderate (w/s = 1.3) and ion aurora mild
- The aurora does not jump between a handful of levels: functional fits improve predictions

# Conclusions

- Diffuse aurora contributes about 3/4 of the precipitating energy flux averaged over all conditions
- Contribution from acceleration rises with higher solar wind input (but remains less than half)
- Wave aurora has the least energy flux, but rises fastest with driving. Wave aurora energy flux most resembles substorms.
- Although nightside dominates energy flux (especially for active conditions), dayside dominates number flux (at least for quiet conditions)